THE BOUNDARY ELEMENT METHOD FOR FLAW CLASSIFICATION IN WAVE GUIDES

S. P. Pelts, J. P. Cysyk and J. L. Rose
Department of Engineering Science and Mechanics
The Pennsylvania State University
114 Hallowell Building
University Park, PA 16802

INTRODUCTION

Guided waves scattered from defects in solid material might contain significant information about those defects. The major goal of non-destructive evaluation is to interpret the ultrasonic signatures from these defects. Scattering of Lamb waves from a normal, surface breaking defect is considered in this study. Reflection and transmission factors of the scattered modes are used to reconstruct the size of the flaws. Scattering Lamb waves from a crack have been investigated in [1-7]. Resonance phenomena for a crack parallel to the plate surface is considered in [5,6]. In this study, the boundary element method combined with the normal mode technique [1,8] is used to study the relationship between crack size and the parameters of the incident mode. Irregular behavior of the reflection coefficient for special parameters of the incident mode is used for size classification.

PROBLEM FORMULATION AND SOLUTION

Let's consider an isotropic elastic plate of unit thickness as shown in Figure 1.

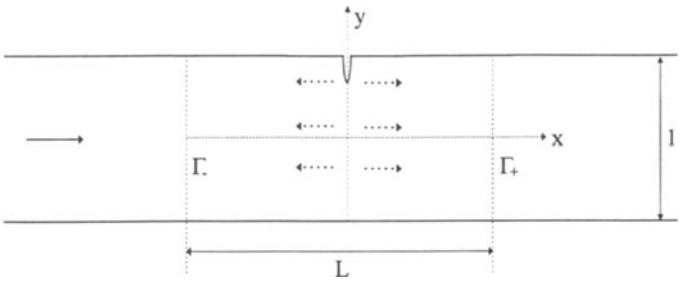

Figure 1. Plate model, solid and dotted arrows show incident and scattered modes respectively.

Review of Progress in Quantitative Nondestructive Evaluation, Vol 16
Edited by D.O. Thompson and D.E. Chimenti, Plenum Press, New York, 1997

The incident wave is a harmonic wave propagating in the positive x direction. The time dependent term $e^{-\iota\omega t}$ is elsewhere omitted, where $\omega = 2\pi f$. The mode incident on the crack results in waves reflected and transmitted of the same order mode and of all other orders of propagation modes which can exist in the plate for the given frequency, according to the phase velocity dispersion curves as shown in Figure 2.

For any frequency, scattering from a crack generates a finite number of propagating and countable nonpropagating modes. The total displacement field is the superposition of the incident and scattered wave fields

$$\mathrm{V} = A_p^{IN}\mathrm{V}_p(y)e^{\iota\alpha_p x} + \sum_{n=1}^{\infty} A_n^{\pm}\mathrm{V}_n(y)e^{\pm\iota\alpha_n x} \tag{1}$$

$$\mathrm{V}_n(y) = \left\{u_1^n(y), u_2^n(y)\right\}, \quad u_1^n(y) = u_x^n(y), \quad u_2^n(y) = u_y^n(y) \tag{2}$$

The A_p^{IN} is the known amplitude of the incident p-th mode, $A_n^{\pm}$ denote the unknown amplitudes of the scattered waves traveling in the positive and negative x directions respectively. $\mathrm{V}_n(y)$ denotes the known displacements of the n-th mode for the traction free plate, α_n represents the corresponding wave numbers.

Far away from a crack only the amplitudes of the propagating waves are significant. The solution of the problem can be obtained by considering only propagation modes in the far scattered field. Therefore, the unbounded plate is replaced with the rectangular area between the dashed lines (Figure 1), for a large enough length L with following boundary conditions Eq. (3-4) on the right and left boundary, Γ_+ and Γ_- respectively, expressed only through propagation modes.

$$\mathrm{V} = A^{IN}\mathrm{V}_p(y)e^{\iota\alpha_p x} + \sum_{n=1}^{N} A_n^{\pm}\mathrm{V}_n(y)e^{\mp\iota\alpha_n L/2} \quad \text{at } \Gamma_{\pm} \tag{3}$$

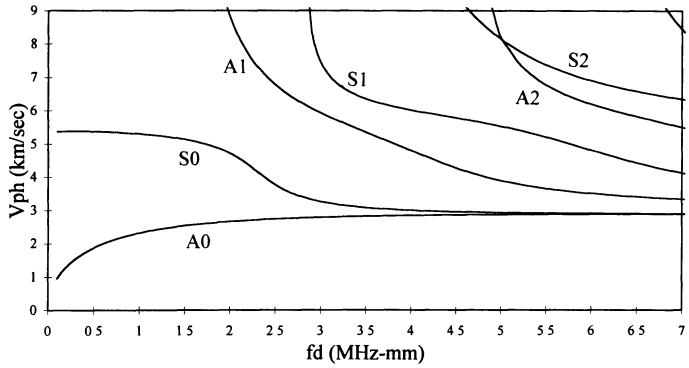

Figure 2. Phase velocity dispersion curves for an aluminum plate with longitudinal velocity V_L=6.3 km/sec, shear velocity V_s=3.1 km/sec.

$$\mathrm{t} = A^{IN}\mathrm{t}_p(y)e^{i\alpha_p x} + \sum_{n=1}^{N} A_n^{\pm}\mathrm{t}_n(y)e^{\mp i\alpha_n x} \qquad \text{at } \Gamma_{\pm} \tag{4}$$

N is the number of propagation modes. The upper sign should be chosen for boundary Γ_+, lower for Γ_-.

$$\mathrm{t}_n(y) = \left\{t_1^n(y), t_2^n(y)\right\}, \quad t_1^n(y) = t_{xx}^n(y), \quad t_2^n(y) = t_{xy}^n(y) \tag{5}$$

$\mathrm{t}_n(y)$ is the n-th stress mode obtained from $\mathrm{V}_n(y)$ by using Hooke's law. The boundary-value problem for modeling area leads to the following boundary integral equations [9].

$$C_{kn}(\xi)u_n(\xi) + \int_{\Gamma} t_{kn}^*(\xi,x)u_n(x)d\Gamma(x) = \int_{\Gamma} u_{kn}^*(\xi,x)t_n(x)d\Gamma(x), \quad \xi \in \Gamma \tag{6}$$

Γ is the total boundary of the modeling area, the value of C_{kl} depends on boundary smoothness, u_l and t_l are boundary values of displacements and tractions. u_{kn}^* and t_{kn}^* are fundamental solutions in the frequency domain [10]. The procedure to obtain a numerical solution of Eq.(5) and to find the reflection and transmission coefficients is discussed in [1,8].

The results presented here are used for a sizing study of a sharp, tiny crack. In order to determine the crack size influence on the scattered elastic field, a frequency range above the cutoff for the first and second antisymmetric modes, A1 and A2 respectively, are considered (Figure 2). First, let's consider frequencies above cutoff for the A1 mode, where for a plate with unit thickness three propagation modes can exist. The thickness of the plate below the crack is $d_1=(1-h) < 1$, where h is crack depth. Such a frequency range is considered by traveling along the A1 branch of the dispersion curve, frequency f_0 is passed, which is the cutoff frequency of A1 for a plate of thickness d_1. In some neighborhood of f_0, the biggest change in the amplitude of the scattered wave field occurs at this critical value f_0. When far enough from this frequency value, the reflection coefficients of the propagation modes do not depend of f_0, because the size d_1 is no longer critical for A1, for this frequency range. The value f_0 is associated with crack depth and from the point of irregular behavior of reflection coefficients, crack size can be estimated. It is well-known that standing waves for the cut off frequencies of odd and even number phase velocity modes have different behavior [11]. Therefore, a similar procedure is obtained by considering the frequencies above the cutoff for the A2 mode. It is shown numerically that different crack sizes are sensitive to different frequency ranges of different modes.

The crack considered has an elliptical shape, with horizontal axis $2s$ and vertical axis $2h$. The relevant crack parameters are sharpness, s/h, and depth, h.

NUMERICAL RESULTS

Reflection coefficients for different incident modes for cracks with depths of 3% and 5% of a plate thickness are plotted in Figures 3-6. In each of these figures there exists a dominant maximum at a particular f_0 frequency value. Crack depth h is calculated on the basis of this f_0 value and the corresponding cutoff frequency f_{cut}. Cutoff frequencies for modes A1 and A2 are 0.5π and 1.5π, respectively [11].

$$h = 1 - \frac{f_{cut}}{f_0} \tag{7}$$

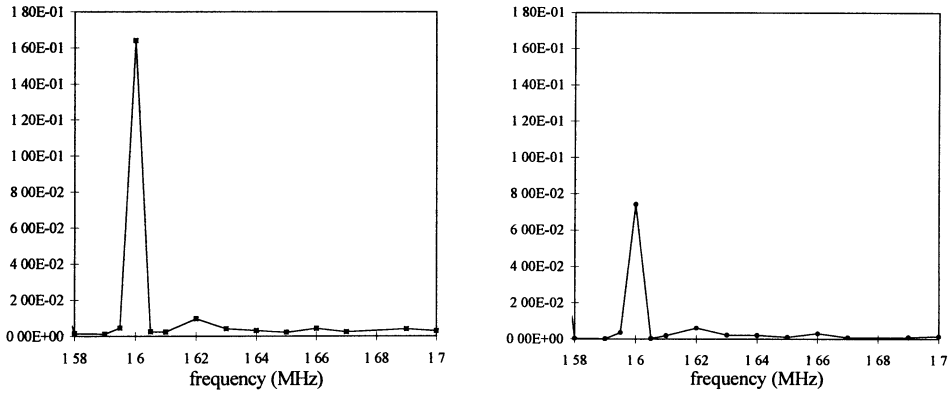

Figure 3. (a) Reflection factors for the A1 scattered mode (b) reflection factors for the S0 scattered mode; both are for the A0 incident mode, crack sharpness $s/h = 0.01$, crack depth h equals 3% of the plate thickness.

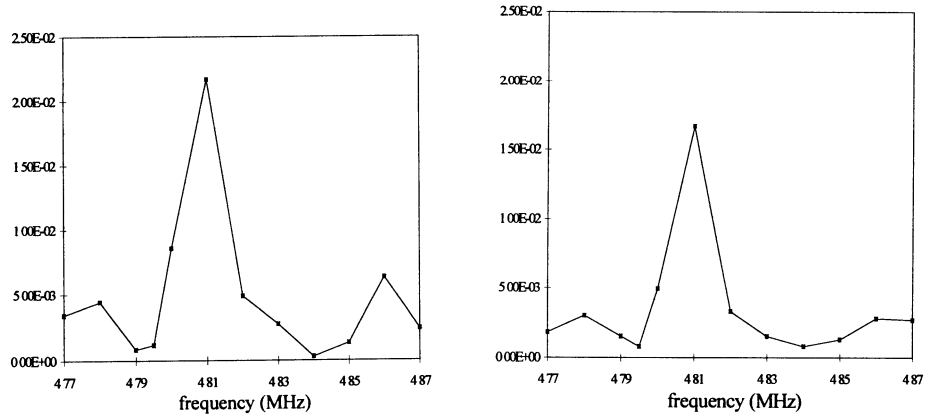

Figure 4. (a) Reflection factors for the S0 scattered mode, (b) reflection factors for the S1 scattered mode; both are for the A2 incident mode, crack sharpness $s/h = 0.01$, crack depth h equals 3% of the plate thickness.

Figures 3-4 represents the solutions of the direct problem for a 3% depth crack for different frequency ranges. The inverse calculation of the crack depth, using Eq. (7) and the data shown in Figure 3, results in a depth of 2.2% of the plate thickness. For the data shown in Figure 4, the inverse calculation results in a crack depth of 2.1% of the plate thickness.

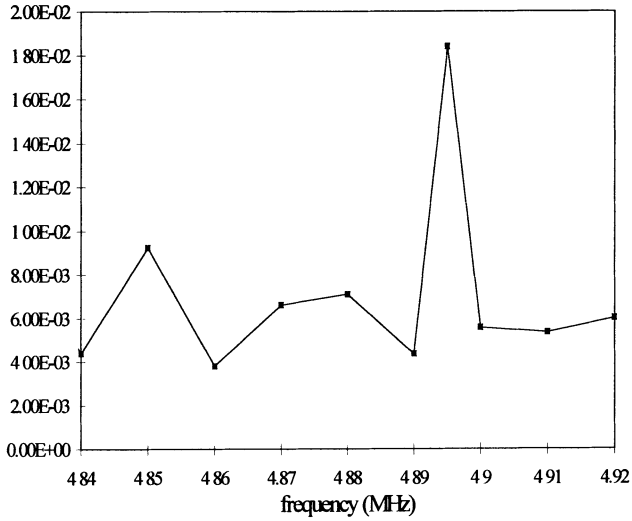

Figure 5. Reflection factors of the A0 scattered mode for the A2 incident mode, crack sharpness $s/h = 0.01$, crack depth h equals 5% of the plate thickness

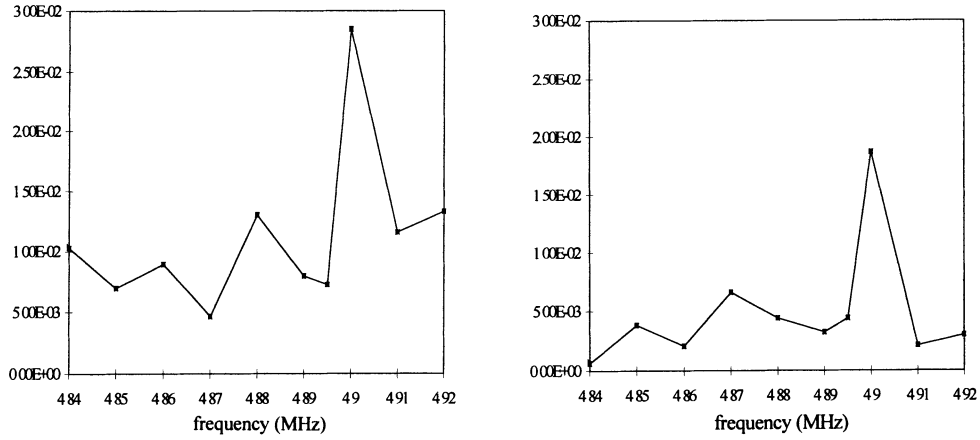

Figure 6. (a) Reflection factors for the A0 scattered mode, (b) reflection factors for the A2 scattered mode; both are for the A0 incident mode, crack sharpness $s/h = 0.01$, crack depth h equals 5% of the plate thickness.

Figures 5-6 show the reflection factors for the 5% depth crack for the cutoff frequency of the A2 modes. The inverse calculation of crack depth, obtained from the data shown in Figure 5, results in a value of 3.7% of the plate thickness. For the data shown in Figure 6, the inverse calculation obtains a crack depth of 3.9% of the plate thickness.

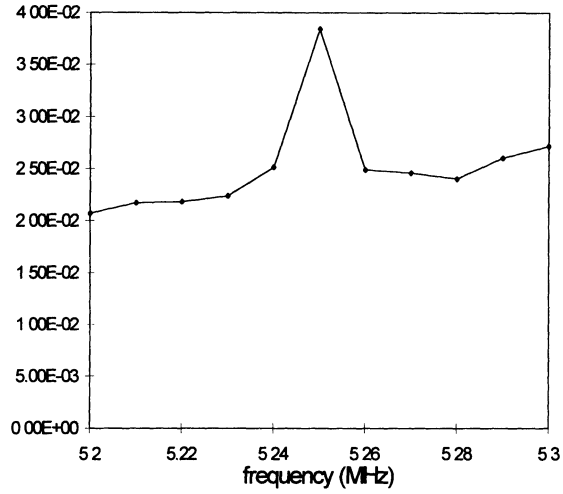

Figure 7. Reflection factors of the A2 scattered mode for the A2 incident mode, crack sharpness $s/h = 0.01$, crack depth h equals 10% of the plate thickness

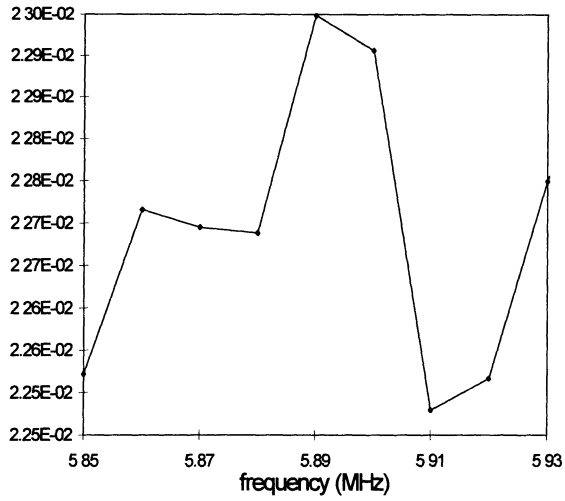

Figure 8. Reflection factors of the A1 scattered mode for the A2 incident mode, crack sharpness $s/h = 0.01$, crack depth h equals 20% of the plate thickness

Figure 7 shows the reflection factors for the 10% depth crack for the cutoff frequency of the A2 mode. The inverse calculation of crack depth results in a value of 10.3% of the plate thickness. Figure 8 shows the reflection factors for the 20% depth crack for the cutoff frequency of the A2 mode. This data results in a calculated crack depth of 20.0% of the plate thickness.

CONCLUDING REMARKS

The algorithm is suggested for classifications of surface breaking cracks with guided waves. There is a frequency value f_0 associated with the depth of the crack. Based on this value of f_0, the inverse calculation for estimating the depth of crack was performed. Inverse calculations based on Eq. (7) gives more precise results for relatively big cracks.

REFERENCES

1. Y. Cho and J. L. Rose, "An elastodynamic hybrid boundary element study on guided wave interactions with a surface breaking crack," *International Journal of Solids and Structures*, (to be published).
2. B. A. Auld and M. Tan, in *IEEE Ultrasonic Symposium Proceedings*, (1978), p.61.
3. M. Tan and B. A. Auld, in *IEEE Ultrasonic Symposium Proceedings*, (1980), p.857.
4. S. K. Datta, Y. Al-Nassar, and A. H. Shah, in *Review of Progress in Quantitative NDE*, Vol. 10, edited by D.O. Thompson and D. Chimenti (Plenum Press, New York, 1991), p. 97.
5. S. I. Rokhlin, *J. Acoust. Soc. Am.*, Vol. 67, No. 4, (1980), p. 1157.
6. S. I. Rokhlin, *J. Acoust. Soc. Am.*, Vol. 69, No. 4, (1981), p. 922.
7. S. Hirose and M. Yamaho, in *Review of Progress in Quantitative NDE*, Vol. 15, edited by D. O. Thompson and D. Chimenti (Plenum Press, New York, 1996), p. 201.
8. Y. Cho and J. L. Rose, *J. Acoust. Soc. Am.*, Vol. 99, No. 4, (1996), p. 2097.
9. Brebbia C. A., Tells J. C. F., and Wrobel L. C., *Boundary Element Techniques*, (Springer, Berlin, 1984).
10. V. D. Kupradze, *Potential Methods in the Theory of Elasticity*, (Israel Program of Scientific Translation, Jerusalem, 1965).
11. K. F. Graff, *Wave Motion in Elastic Solids*, Dover Publications Inc., New York, (1991).